

Modeling of Sporadic-E Structures from Wind-Driven Kelvin-Helmholtz Turbulence

Paul A. Bernhardt

Plasma Physics Division
Naval Research Laboratory
Washington, DC 20375
USA

bern@ppd.nrl.navy.mil

Joseph Werne

Colorado Research Associates Division
NorthWest Research Associates, Inc.
Boulder, CO 80301
USA

werne@cora.nwra.com

Miguel F. Larsen

Department of Physics
Clemson University
Clemson, SC 29634
USA

mlarsen@clemson.edu

ABSTRACT

Atmospheric wind shears control the irregularity structure in the E-region. Near 100 km altitude, where the ion collision frequency is much larger than the ion cyclotron frequency, the degree of shear turning and the direction of maximum shear gradient determine the location of the E-layer peak. The effects of speed shears on the three-dimensional structure of the E-layer are modeled using a system of coupled equations for continuity and momentum that describes both the neutrals and plasma. In the coupled model, the large amplitude components of the neutral wind shear drive the neutral atmosphere unstable and produce Kelvin-Helmholtz (K-H) billows. At the same time, the three-dimensional structure of the same wind shear compresses the ions vertical profile that is not necessarily centered on the node of the wind shear. The shear component is the source of Kelvin-Helmholtz turbulence and it produces quasi-periodic (Q-P) irregularities in the layer along the horizontal direction of the shear. The location of the turbulence in the ions is dependent on the offset lifting or lowering by the turning component of the neutral wind shear. The numerical results of the model study are consistent with the radar and optical observations.

1.0 INTRODUCTION

In the E-region between 90 and 120 km altitude, because the plasma density is one-million times less than the neutral density, neutral wind dynamics plays a controlling role for determining the plasma irregularity structures. Several sources of neutral drivers of E-region irregularities have been proposed including (1) gravity waves [Woodman et al., 1991], (2) plasma instabilities driven directly by neutral wind shears [Cosgrove and Tsunoda, 2003; 2004; Tsunoda and Cosgrove, 2004], and (3) the Kelvin-Helmholtz (KH) instability generated by wind shears that produces turbulence that couples to the plasma [Larsen, 2000; Bernhardt, 2002]. This latter process is described in the next sections. First, the strong evidence of neutral

Bernhardt, P.A.; Werne, J.; Larsen, M.F. (2006) Modeling of Sporadic-E Structures from Wind-Driven Kelvin-Helmholtz Turbulence. In *Characterising the Ionosphere* (pp. 34-1 – 34-14). Meeting Proceedings RTO-MP-IST-056, Paper 34. Neuilly-sur-Seine, France: RTO. Available from: <http://www.rto.nato.int/abstracts.asp>.

Modeling of Sporadic-E Structures from Wind-Driven Kelvin-Helmholtz Turbulence

wind shears near the mesopause and in the lower thermosphere at E-layer altitudes is illustrated with observations of chemical trails. Next, the theory for the development of neutral fluctuations is described with a fluid model. The strength and scale sizes for the turbulence are parameterized by the influence of the wind shear strength through the Richardson number and the viscous damping with the Reynolds number. The coupling of the neutral turbulence to the plasma is described by time-dependent electrodynamic equations. The plasma acts like a self-polarizing tracer of the neutral motion that follows flow driven by the wind but modified by the magnetic field orientation through the Lorentz force.

Observational evidence of the effects the neutral KH instability on E-region densities takes many forms. Using a technique of artificial glow excitation with high power radio waves at the Arecibo HF Facility, Djuth et al. [1999], Kagan et al. [2000] and Bernhardt et al. [2002] have provided images of sporadic-E layers with KH like structures. Earlier, Miller and Smith [1978] used incoherent scatter radar scans to show the formation of KH-like billow structures in the E-layers over Arecibo, Puerto Rico. Larsen [2000] proposes that the shear driven instability in the neutrals may produce electron density structures that seed plasma instabilities that form smaller scale structures. This mechanism has been supported by observational evidence of radar backscatter [Choudhary et al. 2005].

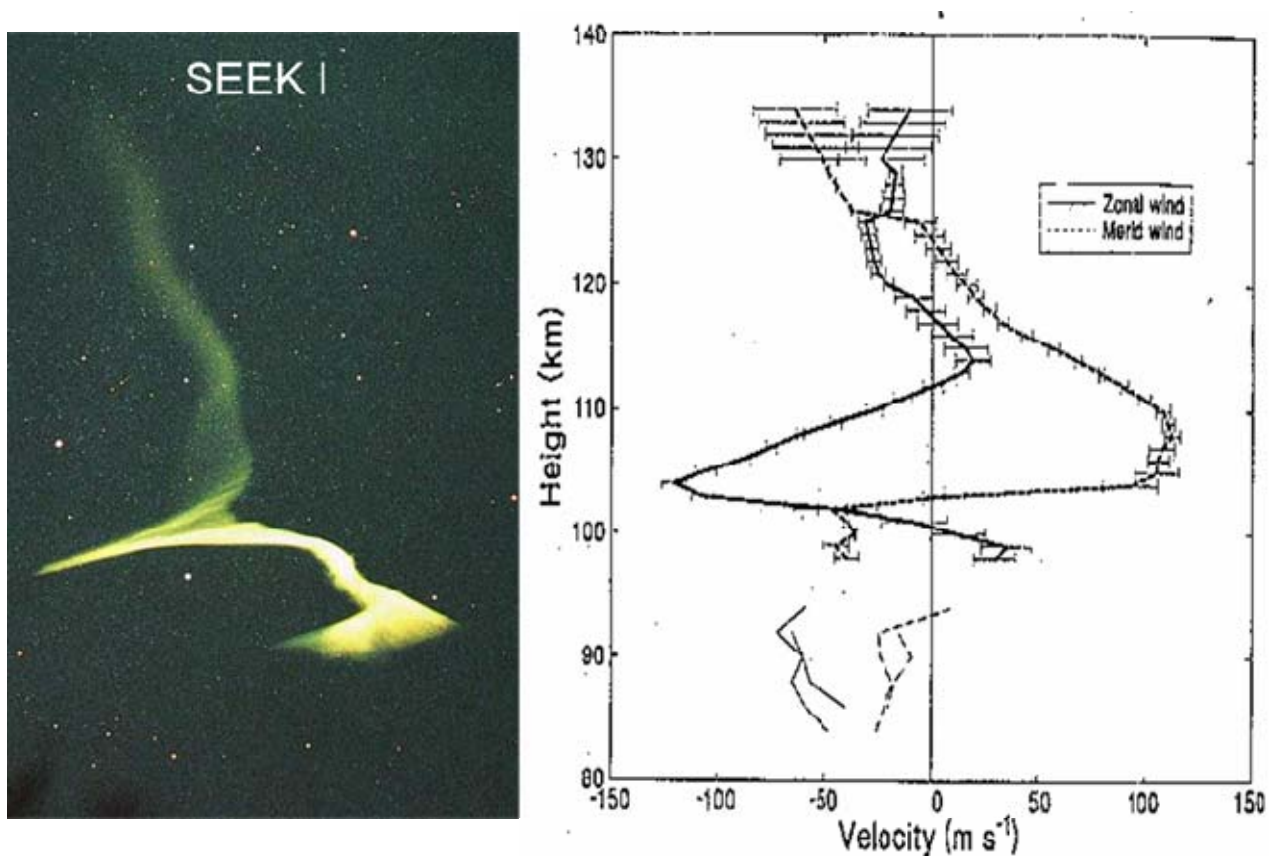


Figure 1: Wind shear derived from a TMA Trail on 20 August 1996, 1530 GMT.

2.0 STRONG SHEARS IN THE MESOSPHERE

At altitudes near 100 km, strong wind shears are found at all latitudes. In a study of chemical release tracer measurements, Larsen [2002] reports that sheared neutral winds have been measured with maximum speeds exceeding 100 m/s over a wide variety of longitudes, seasons, and times of the day. Figure 1 illustrates the distortion of a tri-methyl aluminum (TMA) trail by the large amplitude wind shears. Multiple camera site triangulations are used to derive the horizontal wind vector as function of altitude. Figure 1 also shows such a derived wind profile based on motion of the self-luminous material.

These large amplitude winds have three effects on metallic ion layers of the sporadic-E region. First the shears compress the layers and increase their density [Whitehead, 1989]. The E-layer maximum density forms near the node of the zonal component of the wind shear. Second, the wind shear can drive an interchange instability that ripples the plasma layer [Cosgrove and Tsunoda, 2004]. Third, a strong wind shear becomes unstable yielding billow structures by the Kelvin-Helmholtz instability [Layzer, 1962; Smith and Miller; 1980]. The combination of the three effects produces dense irregular layers near 100 km altitude.

3.0 NON-LINEAR EVOLUTION OF THE NEUTRAL KH INSTABILITY

Dynamics and morphology of a stratified turbulent shear layer in the mesosphere will be examined using hydrodynamic equations governing the hydrodynamic flow of a viscous fluid of varying density and temperature. To simulate the non-linear evolution of the Kelvin-Helmholtz instability and subsequent turbulence dynamics, we begin with the Boussinesq approximation in a Cartesian geometry. A stream background flow

$$u = U_0 \tanh(z/d), \quad v = V_0 \operatorname{sech}(z/d), \quad w = 0$$

is initiated with a constant peak velocity $(U_0, V_0, 0)$, scale-length d , and vertical coordinate z . The background temperature is initially linear: $(T - T_0) = \gamma z$, where γ is the constant mean thermal gradient. The equations of motion describing mass conservation, momentum, heat, are

$$\nabla \cdot \vec{u} = 0, \quad \frac{\partial \vec{u}}{\partial t} + (\vec{u} \cdot \nabla) \vec{u} = \frac{\mu}{\rho_0} \nabla^2 \vec{u} - \frac{1}{\rho_0} \nabla P + \vec{g} \left(1 + \frac{\delta \rho}{\rho} \right)$$

$$\frac{\partial T}{\partial t} + \vec{u} \cdot \nabla T = \kappa \nabla^2 T \quad \text{where } \delta \rho = -\rho_0 \alpha (T - T_0)$$

Here $\vec{u} = (u, w, v)$ and $\vec{x} = (x, y, z)$ are velocity and position vectors, α is the thermal expansion coefficient, κ is the thermal diffusivity, and \vec{g} is the acceleration due to gravity. These equations have been solve numerically in 3D [1] for high Reynolds numbers ($Re = U_0 h / \nu = 2500$) for a planer speed shear with $V_0 = 0$ to give the turbulent flow shown in Figure 2.

The turbulent mixing generated by the Kelvin-Helmholtz (KH) instability in the mesosphere will use the same numerical simulation model with a more realistic input for the wind shear. The ratio of out-of-plane to in-plane wind speed is given by the parameter $\beta = V_0 / U_0$. A pure planer shear has $\beta = 0$ and as β approaches 1 the shear turns into a pure turning shear (Figure 3). The measured wind shears in the mesosphere typically are described with a β between 0.7 and 1.0. No previous KH simulations have been performed in this parameter range.

Modeling of Sporadic-E Structures from Wind-Driven Kelvin-Helmholtz Turbulence

The Reynolds number for these simulations will vary between about 3000 at 100 km altitude and 300 at 120 km altitude. The lower Reynolds number simulations will be less turbulent than those shown in Figure 1. Exploration of the neutral dynamics for a turning shear for a variety of Reynolds numbers will be the objective of future modeling.

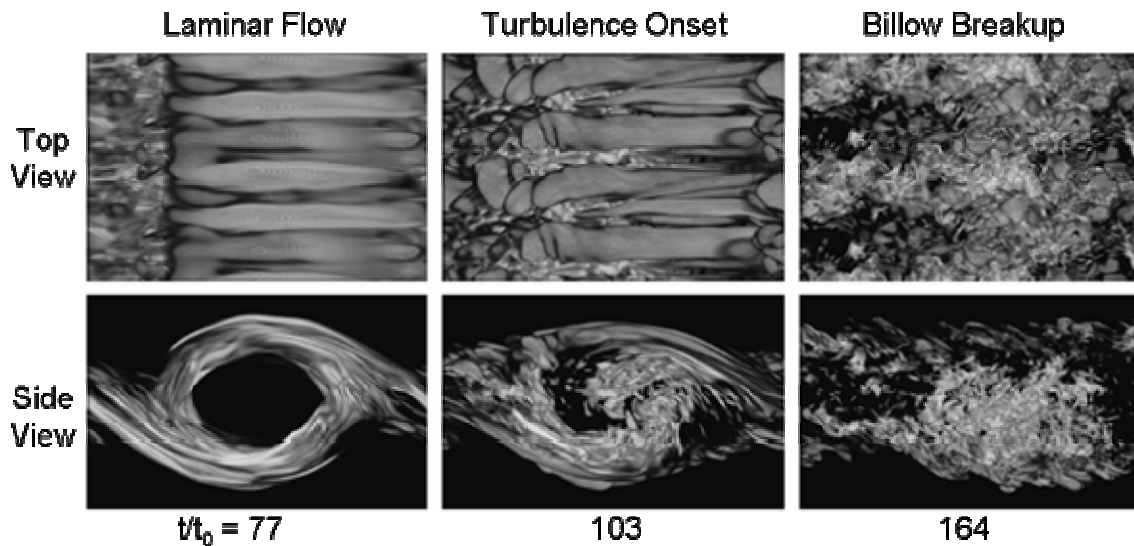


Figure 2: Neutral stratified shear turbulence for a planer speed shear. The parameters for the simulation are Richardson Number $Ri = 0.05$ and Reynolds Number $Re = 2500$ [Reif, Werne, Andreassen, Meyer, Davis-Mansour, 2002]. The time scale for the figure is the shear scale divided by the maximum wind speed (d/U_0) which is on the order of 20 seconds.

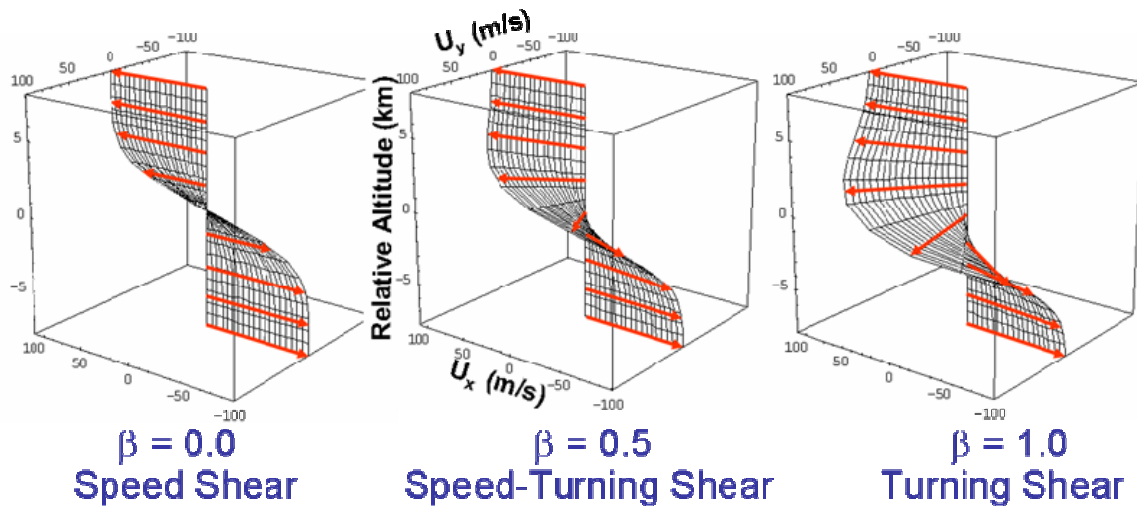


Figure 3: Types of neutral velocity shears. Each shear has the same altitude profile for the x-directed velocity.

4.0 COUPLING TO THE E-REGION PLASMA

The plasma density in the ionosphere is described by the continuity equation

$$\frac{\partial n_{i,e}}{\partial t} + \nabla \cdot (n_{i,e} \mathbf{v}_{i,e}) = - \begin{cases} \beta_i n_i \rho/m \\ \alpha_e n_i n_e \end{cases}$$

where $n_{i,e}$ is the electron or ion density depending on subscript, $\mathbf{v}_{i,e}$ is the velocity vector, ρ is the neutral mass density, m is the neutral particle mass, β_i is the ion-molecule charge exchange rate, α_e is the ion-electron recombination rate. The quantities in red will be affected by fluctuations in the neutral atmosphere produced by the KH instability. The terms on the right side of the continuity equation represent chemical reactions which affect the plasma density by changing the composition. The transport flux $n_{i,e} \mathbf{v}_{i,e}$ causes density fluctuations through plasma motion and compression.

An external force on the plasma yields transport by interactions with the background magnetic field and collisions. For a steady state velocity without inertia, the velocity is related to the force through ion and electron mobility tensors $\boldsymbol{\kappa}_{i,e}$

$$\mathbf{v}_{i,e} = \boldsymbol{\kappa}_{i,e} \cdot \mathbf{F}_{i,e}$$

$$\text{where } \boldsymbol{\kappa}_{i,e} = \begin{bmatrix} k_{1i,e} & k_{2i,e} & 0 \\ -k_{2i,e} & k_{1i,e} & 0 \\ 0 & 0 & k_{0i,e} \end{bmatrix} \text{ has the components}$$

$$k_{0i,e} = \frac{1}{m_{i,e} \nu_{i,en}}, \quad k_{1i,e} = \frac{1}{m_{i,e} \nu_{i,en}} \frac{\nu_{i,en}^2}{\nu_{i,en}^2 + \Omega_{i,e}^2}, \quad k_{2i,e} = \frac{1}{m_{i,e} \nu_{i,en}} \frac{\nu_{i,en} \Omega_{i,e}}{\nu_{i,en}^2 + \Omega_{i,e}^2}$$

with $\nu_{i,en}$ as the ion/electron neutral collision frequency and the gyro frequencies given by

$$\Omega_{i,e} = \frac{q_{i,e} B}{m_{i,e}}$$

These equations are written in the reference frame of the background magnetic field. Often it is useful to translate the plasma equations into the reference frames of the local vertical direction and the direction of the wind shear. The vertical and wind direction- coordinate transformations will be called \mathbf{T} and \mathbf{S} , respectively. With these transformations the mobility tensor becomes

$$\mathbf{A}_{i,e} = -\mathbf{S} \cdot (\mathbf{T} \cdot \boldsymbol{\kappa}_{i,e} \cdot \mathbf{T}^{-1}) \cdot \mathbf{S}^{-1}$$

The forces on the plasma are written as

$$\mathbf{F}_{i,e} = q_{i,e} \mathbf{E} + m_{i,e} \nu_{i,en} \mathbf{U}_T - \nabla p_{i,e} / n_{i,e}$$

Modeling of Sporadic-E Structures from Wind-Driven Kelvin-Helmholtz Turbulence

where the pressure $p_{i,e} = n_{i,e} k T_{i,e}$ and \mathbf{U}_T is the neutral flow velocity vector. The wind is highlighted in red to indicate direct coupling to the KH turbulence.

The plasma force acts through the mobility tensor to yield the velocity components for the ions and electrons as

$$\mathbf{v}_i = \mathbf{A}_i \cdot \left(\frac{kT}{n} \nabla n + e \nabla \phi \right) - m_i v_i \mathbf{A}_i \cdot \mathbf{U}_T$$

$$\mathbf{v}_e = \mathbf{A}_e \cdot \left(\frac{kT}{n} \nabla n - e \nabla \phi \right) - m_e v_e \mathbf{A}_e \cdot \mathbf{U}_T$$

where ϕ is the electrostatic potential from charge separation.

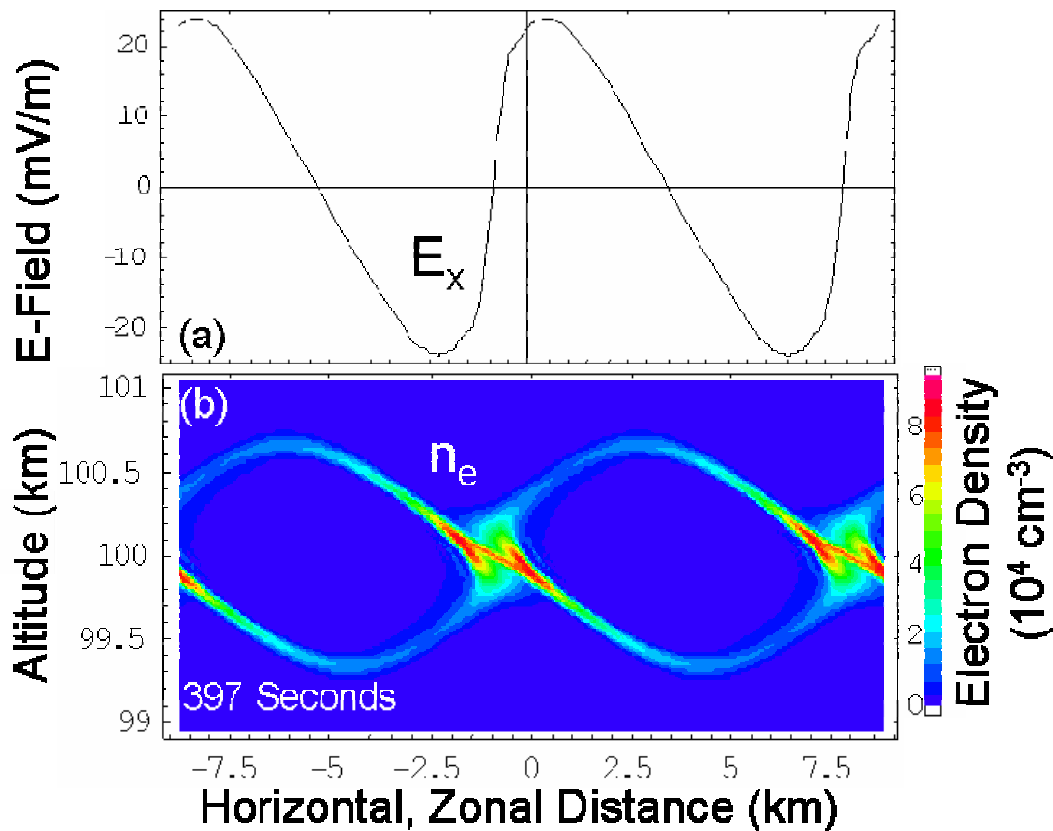


Figure 4: Intermediate stage for the distortion of the E-layer densities and electric fields with the KH instability responding to a neutral speed shear in the zonal direction.

Finally the continuity equation relates the plasma velocity changes to the changes in plasma density. Assuming quasi neutrality, the time dependent equation for the ion and electron densities becomes

$$\frac{\partial n}{\partial t} = -\nabla \cdot [\mathbf{A}_i \cdot (k T \nabla n + e n \nabla \phi)] + \nabla \cdot (m_i v_i n \mathbf{A}_i \cdot \mathbf{U}_T)$$

$$\frac{\partial n}{\partial t} = -\nabla \cdot [\mathbf{A}_e \cdot (k T \nabla n - e n \nabla \phi)] + \nabla \cdot (m_e v_e n \mathbf{A}_e \cdot \mathbf{U}_T)$$

The electric potential is found by equating these two equations with the result

$$\nabla \cdot [e n (\mathbf{A}_i + \mathbf{A}_e) \cdot \nabla \phi] = \nabla \cdot [kT(\mathbf{A}_e - \mathbf{A}_i) \cdot \nabla n] + \nabla \cdot [n(m_i v_i \mathbf{A}_i - m_e v_e \mathbf{A}_e) \cdot \mathbf{U}_T]$$

To determine the evolution of the E-layer plasma under the influence of a neutral KH turbulence, the ion continuity equation is solved using a neutral wind driver and the self consistent electric potential. The details of the solution of these equations in two-dimensions are described by Bernhardt [2002].

5.0 SIMULATION OF 2D TURNING SHEAR DYNAMICS

The previous work by Bernhardt [2002] focused on two-dimensional simulations of E-layer structures for speed shears at 100 and 120 km altitude where the shear direction was in the east-west, zonal direction. The resulting plasma structures were anti-symmetric layers or clumps centered on the nodes of the Kelvin-Helmholtz billows (Figure 4). The layer eventually divides into two rippled layers on either side of the KH billow.

For the new simulations presented here, a turning shear is used to develop the KH-structures in the neutrals and the neutral transport is used to drive the E-layer plasma in an oblique, non-zonal plane. The simulation starts with the profiles for the neutral wind shear and initial plasma densities shown in Figure 5. A turning shear with $\beta = 1$ drives the KH instability with the maximum shear located at an angle of 59 degrees with the geographic meridian. The amplitudes of the wind components are $U_0 = V_0 = 100$ m/s. Under these conditions, the steady state plasma layers forms near 100.4 km above the node of the neutral wind at 100 km. This is a characteristic of the E-layer where $\Omega_{ci} \ll v_i$.

The numerical simulation will use parameters appropriate to the mesopause region at 100 km altitude. The scale height for the background atmosphere $H_0 = 5.4$ km. The wind shear has scale length $d = 700$ m. With these parameters, the KH instability growth time is about 100 seconds and the characteristic simulation time

$d/U_0 = 17$ seconds. The Richardson number ($Ri = \frac{g d^2}{H_0 U_0^2}$) is 0.08 which is less than the critical value of

0.25 for the KH instability. The Reynolds number ($Re = \frac{\rho_0 d U_0}{\mu}$) is 3480 indicating that in three-

dimensions, the flow will resemble Figure 1. The simulations presented here are only 2-dimensional in the plane of the strongest shear so that only laminar billows will form in the neutral densities.

Modeling of Sporadic-E Structures from Wind-Driven Kelvin-Helmholtz Turbulence

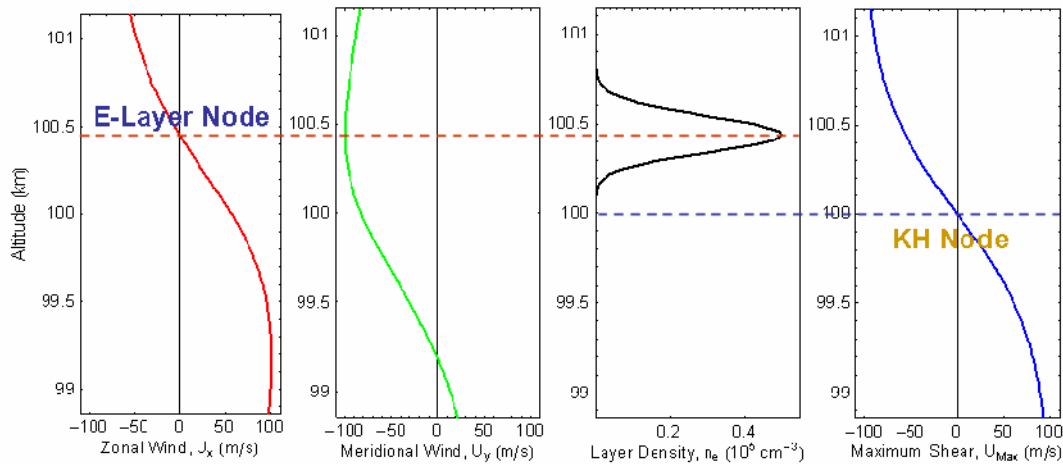


Figure 5: Neutral wind components and E-layer profiles at the start of the two-dimensional simulation of neutral KH instability coupling to the plasma layer near 100 km altitude.

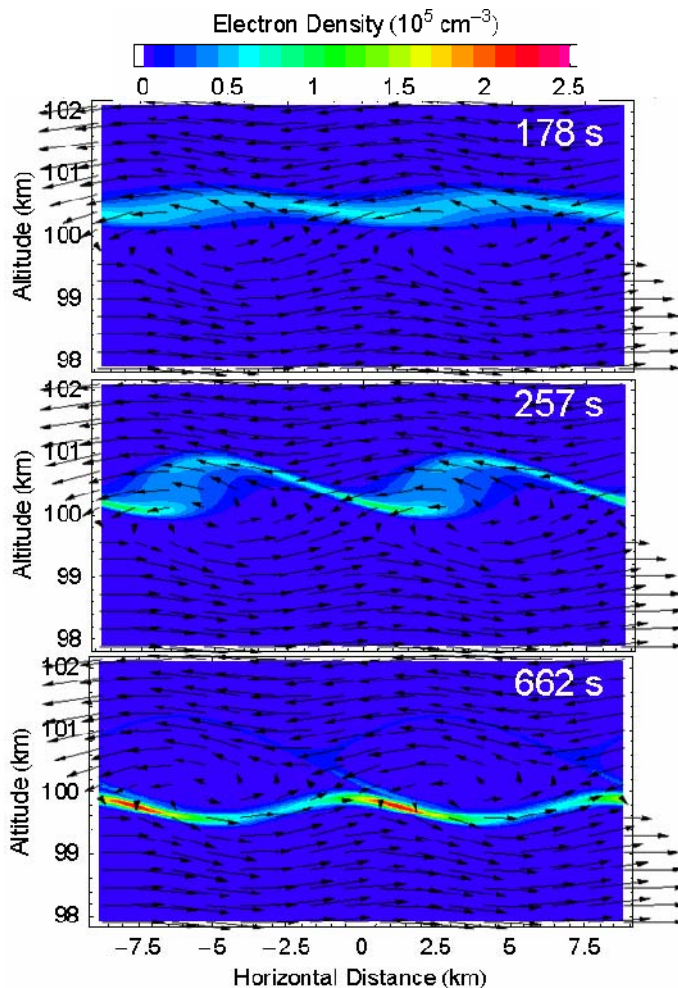


Figure 6: Break up of the E-layer by neutral KH billows. The neutral wind vectors (black arrows) disturb the horizontal structure of the layer by transporting and compressing plasma to lower altitudes.

A sample of the coupled neutral KH and plasma electrodynamic simulation is given in Figure 6. The ion flow induced by the neutral wind does not follow the wind vectors but responds to both internally generated electric fields and ion-neutral coupling. The horizontal layer becomes a rippled layer that never completely reaches steady state. The density of the layer goes from an initial peak density of $0.5 \times 10^5 \text{ cm}^{-3}$ to over $2 \times 10^5 \text{ cm}^{-3}$ as it responds to the neutral KH flow. During this process, the strength of the polarization electric fields becomes greater than 60 mV/m.

The morphology of the E-layer by the turning shear illustrated by Figure 6 is different from that produced by the speed shear shown in Figure 4 and discussed by Bernhardt [2002]. For identical atmospheric conditions, the speed shear splits the layer into two rippled layers separated by the billow height. By comparison, the full turning shear causes the flat layer to evolve from its equilibrium altitude near 100.4

km to a new, rippled structure near 99.6 km average altitude. A static equilibrium state was not found with the simulation but there seems to be periodic convection of the high density region along the bottom of the neutral billows to yield a dynamic equilibrium. By adjusting the turning shear parameter, the E-layer can be made to split into two layers with one layer containing more total density than the other. Observational evidence of such an asymmetric layer splitting has been reported by Miller and Smith [1978].

The introduction of the parameterized turning/speed shear provides a wider family of responses to the wind by the E-layer than obtained with the speed shear. Even more types of structures will develop with a fully three-dimensional turbulent wind. The two-dimensional simulations only hint at the full scale dynamics produced by the full three-dimensional KH instability. In two-dimensions, the KH billows are laminar and this structure is reflected in the electron densities. In three-dimensions, the turbulence driven by the wind shear will cause the billow to breakup into fine scale irregularities which will be mirrored in the E-layer densities. When the KH-wave structure are present in the neutral atmosphere, the plasma responds as an electrodynamic tracer. The KH wind component can also drive small scale plasma field aligned irregularities by the gradient drift, plasma interchange instability (GDI) for the electric fields set up in the plasma may drive currents for the Farley-Buneman, two-stream instability (FBI). These irregularities can be detected using radar scatter.

6.0 EXPERIMENTAL CONFIRMATION OF THE KH STRUCTURING PROCESS IN THE E-REGION

A number of ground and space-based diagnostics have produced data which are consistent with (1) a neutral wind shear exciting the KH instability in the mesosphere and (2) coupling of the KH turbulence to the plasma to form sporadic-E irregularities. During the second Sporadic-E Experiment over Kyushu (SEEK2), a number of new measurements were made of the neutral and plasma environment associated with a sporadic-E event. Using a tri-methyl aluminum (TMA) trail Larsen et al. [2005] were able to trace the neutral atmosphere motion showing both strong wind shears Kelvin-Helmholtz billows in the 102 to 108 km altitude range (Figure 7). The horizontal wavelength was approximately 5 km and the vertical wavelength was approximately 2 km. These billows resemble the early-time, side-view results for the simulations in Figure 1. These wind shears were characterized by low Richardson numbers which are KH unstable.

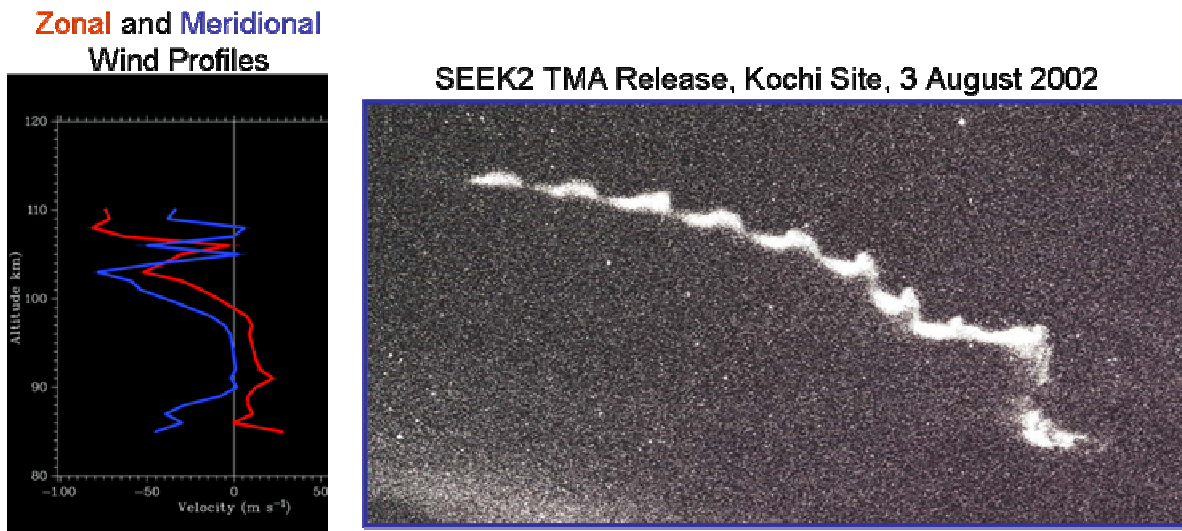


Figure 7: Upleg portion of the TMA trail during the SEEK2 experiment.

Modeling of Sporadic-E Structures from Wind-Driven Kelvin-Helmholtz Turbulence

The downleg of the SEEK2 rocket provided observations of strong turbulence and complete breakup of of the TMA trail (Figure 8). The measured wind shears were characterized by very low Richardson numbers and a neutral dispersal of the TMA that resembles the late time turbulence illustrated in Figure 1.

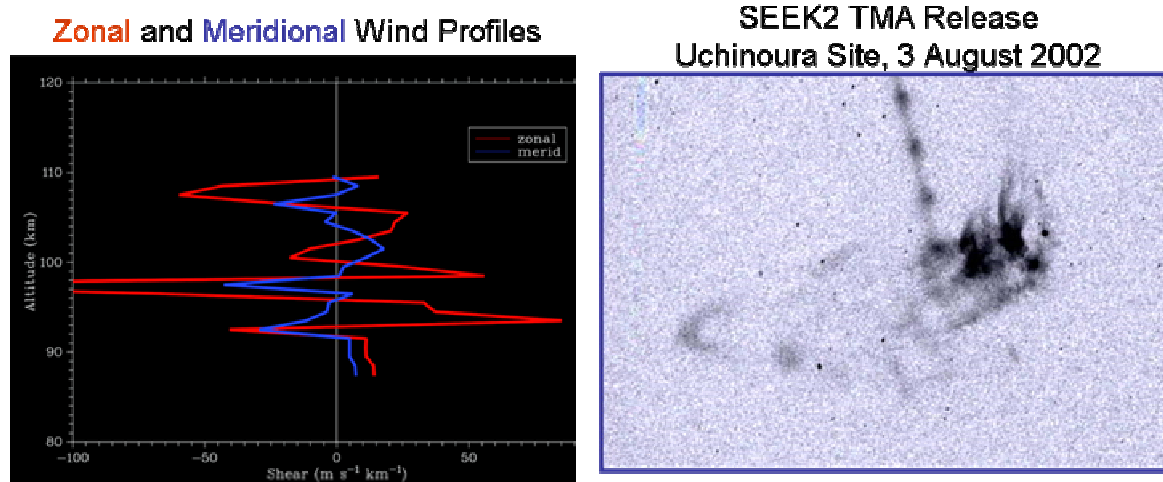


Figure 8: Downleg portion of the TMA trail during the SEEK2 experiment.

Two-dimensional E-layer density imaging was provided by a radio tomography experiment that was flown on the SEEK2 rockets by Bernhardt et al. [2005]. The radio transmissions from the rocket were received on the ground to yield the integrated electron density from the rocket as it passed over the E-region. A tomographic image was formed from the TEC data assuming that the plasma layer was stable throughout the rocket flight (Figure 9). The E-region plasma density image shows a separation of the layer that is similar to the model results produced by the electrostatic simulation illustrated in Figure 6.

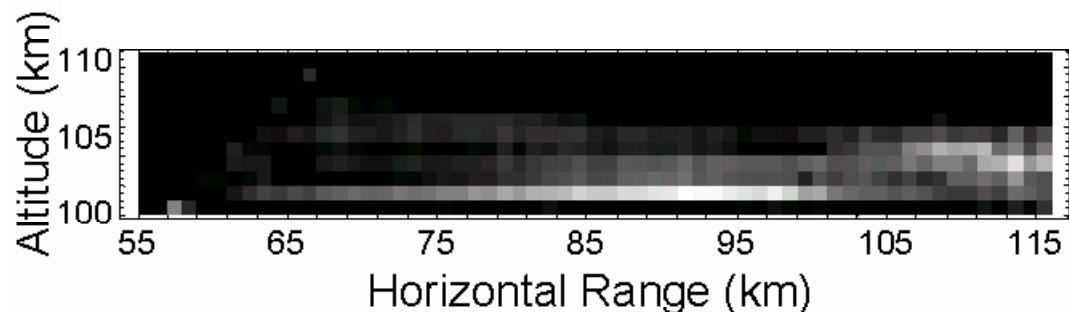


Figure 9: High resolution tomographic image of the E-layer recorded during the SEEK2 experiment.

Numerous other data were recorded during the SEEK2 experiments using in situ plasma and electric field probes, ground based radars and cameras, etc. All the SEEK2 measurements showed the evidence of irregularities that could be attributed to KH turbulence in the neutrals driving the plasma. Yamamoto et al. [2005] show that the VHF radar recorded quasi-periodic backscatter echoes that have KH-like distances between regions of strong backscatter (Figure 10).

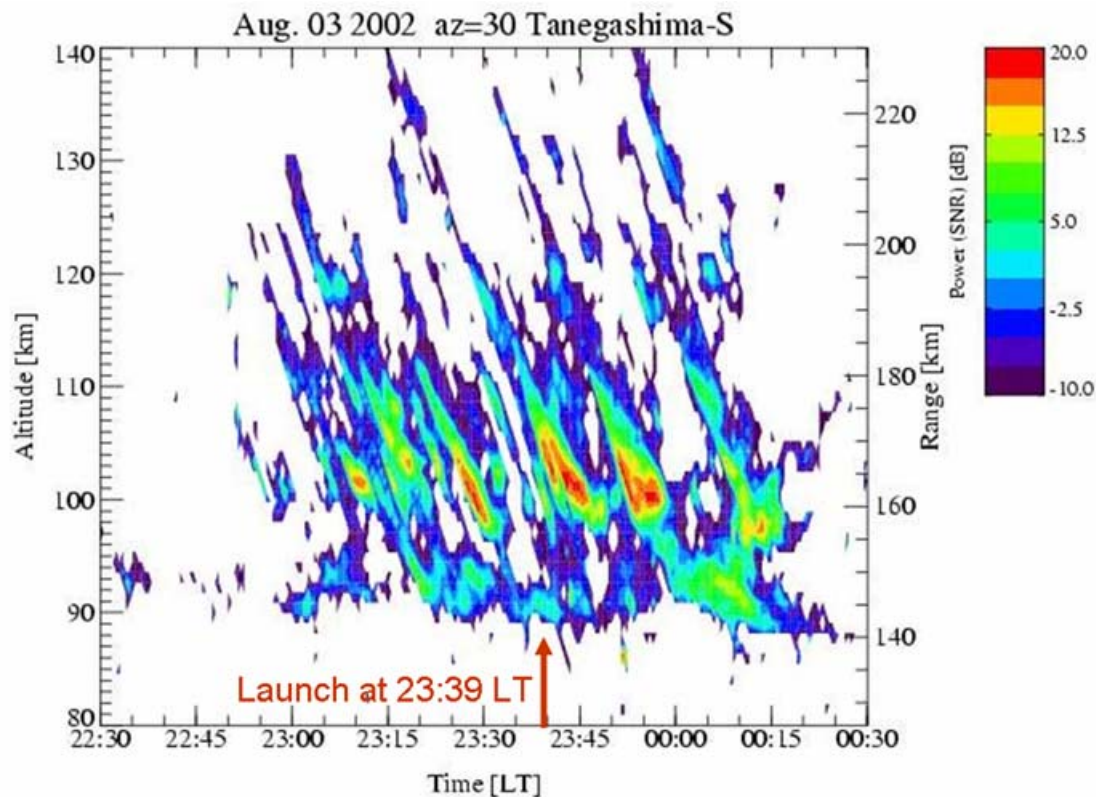


Figure 10: High HF radar quasi-periodic echoes at the time of the launch of SEEK2 rocket.

7.0 DISCUSSION

This paper has focused on neutral turbulence as a source of structure in the E-region but it is useful to consider the effects of the Cosgrove and Tsunoda (CT) plasma instability for comparison. The growth rate for the CT instability is a maximum along an azimuth that is 45 degrees to the direction of the magnetic meridian. At this angle, the CT instability has the property that any perturbation in the thin plasma layer gets amplified to form multiple E layer density structures. Figure 22, adapted from Tsunoda and Cosgrove [2004], illustrates the results for a two-dimensional, numerical simulation of the Cosgrove/Tsunoda (CT) instability. Both density and electric field structures are generated by the shear driven plasma instability. A comparison of the second panel in Figure 6 and the top panel of Figure 11 shows that the two instabilities can yield similar splitting of the E-layer. As mentioned previously, this type of splitting was measured using radio beacon tomography technique as shown on the right half of Figure 9. To determine which process is acting at a given instant, the differences between the mechanisms (Neutral KH versus Plasma CT) should be explored.

The primary differences between the plasma CT instability and the neutral KH instability are subtle. Both instabilities produce plasma structures that can locally split the E-region into two layers. The KH instability provides periodic structures with a specific wave number at any orientation relative to the meridian. The CT instability provides periodic structures at any wave number with a specific (40 degree) azimuth to the magnetic meridian. The KH neutral mode may distort the layer which then could be a seed for the CT instability. Both neutral KH and plasma CT instability may be acting simultaneously.

Modeling of Sporadic-E Structures from Wind-Driven Kelvin-Helmholtz Turbulence

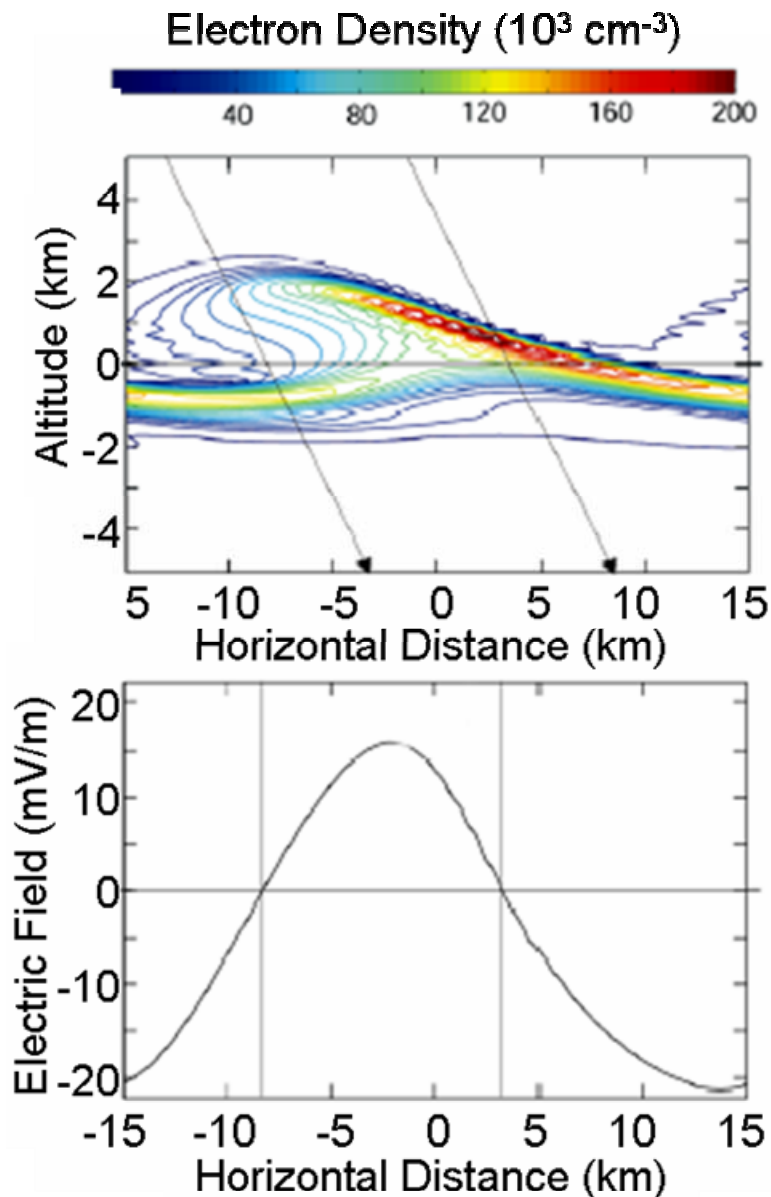


Figure 11: Sporadic-E layer distortion produced by CT instability at $t = 522$ seconds. The oblique arrows are the magnetic field projected into the solution plane.

For large Reynolds numbers, the KH instability should couple much finer scale turbulence to the plasma than has been reported in the simulations of the E-Layer plasma instability by Cosgrove and Tsunoda [2003]. The reason for this is that the KH instability launches three-dimensional turbulence whereas the plasma CT mode is a two-dimensional instability.

In summary, the evidence for KH modulation of E-Layer is compelling but not definitive. Unstable wind shears have been seen using both TMA releases and LIDAR observations. Neutral turbulence has been

directly observed by dispersal of TMA trails. The turbulence level is consistent with the low Richardson number derived from the wind shear. A $Ri \sim 0.2$ matches the observed KH billows and the $Ri \sim 0.02$ matches the strong turbulence from SEEK2 [Larsen et al., 2006]. Other references that measure electron density images show both billows and longitudinal tubes that are consistent with the KH picture (Djuth et al. [1999], Kagan et al. [2000] and Bernhardt et al. [2002]) and billows are observed using incoherent scatter scans [Miller and Smith, 1978; Hysell et al., Larsen, 2004]. The SEEK2 tomographic Image by Bernhardt et al. [2996] shows layer separation that can be attributed to the neutral KH instability. Future model studies and observational experiments need to be conducted to reconcile the contribution of neutral KH to sporadic-E irregularities.

8.0 REFERENCES

- [1] Bernhardt, P.A., The Modulation of Sporadic-E Layers by Kelvin-Helmholtz Billows in the Neutral Atmosphere, **J. Atm. Solar Terr. Phys.**, **54**, 1487-1504, 2002.
- [2] Bernhardt, P.A., CA Selcher, CL Siefring, M Wilkens, C Compton, M Yamamoto, S Fukao, T Ono, M Wakabayashi, H Mori, Radio Tomographic Imaging of Sporadic E-Layers During SEEK2, **Annales Geophysicae**, **23**, 2357-2368, 2005.
- [3] Bernhardt, P.A., C. A. Selcher, C. L. Siefring, E. Gerken, Glow Imaging of Ionospheric Density Structures and Plasma Drifts with Artificial Illumination by High Power Radio Waves, **IEEE Trans. Plasma Sci.**, **33**, 504-505, 2005
- [4] Choudhary RK, JP St Maurice, LM Kagan, KK Mahajan, Quasi-periodic backscatters from the E region at Gadanki: Evidence for Kelvin-Helmholtz billows in the lower thermosphere Source: **J. Geophys. Res.**, **110**: Art. No. A08303,2005
- [5] Cosgrove, R. B., and R. T. Tsunoda (2003), Simulation of the nonlinear evolution of the sporadic-E layer instability in the nighttime midlatitude ionosphere, **J. Geophys. Res.**, **108**, 1283, doi:10.1029/2002JA009728
- [6] Cosgrove RB, RT Tsunoda, Instability of the E-F coupled nighttime midlatitude ionosphere, **J. Geophys. Res.**, **109**, Art. No. A04305, 2004
- [7] Djuth, F.T., P.A. Bernhardt, C.A. Tepley, J.A. Gardner, M.C. Kelley, A.L. Broadfoot, L.M. Kagen, M.P. Sulzer, J.H. Elder, B. Isham, C. Brown, and H.C. Carlson, Production of large airglow enhancements via wave-plasma interactions in Sporadic-E, **Geophys. Res. Lett.**, **26**, 1557-1560, 1999.
- [8] Hysell DL, Larsen MF, Zhou QH, Common volume coherent and incoherent scatter radar observations of mid-latitude sporadic E-layers and QP echoes, **Annales Geophys.** **22**, 32770329, 2004.
- [9] Kagan, L.M., MC Kelley, F. Garcia, PA Bernhardt, FT Djuth, MP Sulzer, CA Tepley, The structure of electromagnetic wave-induced 557.7-nm emission associated with a sporadic-E event over Arecibo, **Physical Review Letters**, **85**, 218-221, 3 July 2000.
- [10] Larsen M.F., A shear instability seeding mechanism for quasiperiodic radar echoes, **J. Geophys. Res.**, **105**, 24931-24940, 2000.

Modeling of Sporadic-E Structures from Wind-Driven Kelvin-Helmholtz Turbulence

- [11] Larsen MF, Winds and shears in the mesosphere and lower thermosphere: Results from four decades of chemical release wind measurements, **J. Geophys. Res. – Space Phys.**, **107** (A8): Art. No. 1215, 2002.
- [12] Larsen MF, Yamamoto M, Fukao S, Tsunoda RT, Saito A, Observations of neutral winds, wind shears, and wave structure during a sporadic-E/QP event, , **Annales Geophysicae**, **23**, 2369-2375, 2005.
- [13] Layzer, D., The Turbulence Criterion in Stably Stratified Shear Flow and the Origin of Sporadic E, **Ionospheric Sporadic-E**, E.K. Smith and S Matsushita, Eds., Macmillan, New York, 1962.
- [14] Miller K.L., L.G. Smith, Incoherent-scatter radar observations of irregular structure in the mid-latitude sporadic-E layers, **J. Geophys. Res.**, **83**, 3761-3775 1978.
- [15] Reif BAP, J Werne, Å Andreassen, C Meyer, M Davis-Mansourz, Entrainment-zone restratification and flow structures in stratified shear turbulence, **Center for Turbulence Research, Proceedings of the Summer Program**, pp 245-256, 2002.
- [16] Smith, L.G., and K.L. Miller, Sporadic-E Layers and Unstable Wind Shears, **J. Atm. Terr. Phys.**, **42**, 45-50, 1980.
- [17] Tsunoda, RT, and RB Cosgrove, Azimuth-dependent Es layer instability: A missing link found, **J. Geophys. Res.**, **109**, A12303, doi:10.1029/2004, 2004
- [18] Whitehead, J.D., Recent work on mid-latitude and equatorial sporadic E, **J. Atmos. Terr. Phys.**, **51**, 401-424, 1989.
- [19] Woodman, R. F., M. Yamamoto, and S. Fukao (1991), Gravity wave modulation of gradient drift instabilities in mid-latitude sporadic E irregularities, **Geophys. Res. Lett.**, **18**, 1197– 1200.
- [20] Yamamoto M, Fukao S, Tsunoda RT, Pfaff R, Hayakawa H, SEEK-2 (Sporadic-E Experiment over Kyushu 2) - Project outline, and significance, **Annales Geophysicae**, **23**, 2295-2305 2005.
- [21] Yokoyama, T, T Horinouchi, M Yamamoto, S Fukao, Modulation of the midlatitude ionospheric E region by atmospheric gravity waves through polarization electric field, **J. Geophys. Res.**, **109**: Art. No. A12307, 2004.